J. Appl. Numer. Optim. 7 (2025), No. 3, pp. 309-332 Available online at http://jano.biemdas.com https://doi.org/10.23952/jano.7.2025.3.03

THE TOPOLOGICAL DERIVATIVE METHOD FOR OPTIMUM SHAPE DESIGN AND CONTROL OF GAS NETWORKS

MICHAEL SCHUSTER^{1,*}, JAN SOKOLOWSKI^{2,3,4}

¹Department of Mathematics, Friedrich-Alexander-Universität Erlangen-Nürnberg (FAU), Cauerstr. 11, 91058 Erlangen, Germany ²Institut Élie Cartan de Lorraine, CNRS, UMR 7502, Université de Lorraine, B.P. 70239, 54506 Vandoeuvre-lès-Nancy Cedex, France ³Systems Research Institute of the Polish Academy of Sciences, ul. Newelska 6, 01-447 Warszawa, Poland ⁴Department of Scientific Computing, Informatics Center, Federal University of Paraiba, Brazil

Abstract. In this paper, topological derivatives are defined and employed for gas transport networks governed by nonlinear hyperbolic systems of PDEs. The concept of topological derivatives of a shape functional is introduced for optimum design and control of gas networks. First, the dynamic model for the network is considered. The cost for the control problem includes the deviations of the pressure at the inflow and outflow nodes. For dynamic control problems of gas networks when the turnpike property occurs, the synthesis of control and optimum design of the network can be simplified. That is, the design of the network can be performed for optimal control of the steady-state network model. The cost of design is defined by the optimal control cost for the steady-state network model. The topological derivative of the design cost, given by the optimal control cost with respect to the nucleation of a small cycle, is determined. Tree-structured networks can be decomposed into single network junctions. The topological derivative of the design cost is systematically evaluated at each junction of the decomposed network. This allows for the identification of internal nodes with negative topological derivatives, where replacing the node with a small cycle leads to an improved design cost. As the set of network junctions is finite, the iterative procedure is convergent. This design procedure is applied to representative examples and it can be generalized to arbitrary network graphs. A key feature of such modeling approach is the availability of exact steady-state solutions, enabling a fully analytical topological analysis of the design cost without numerical approximations.

Keywords. Gas networks; Optimum design; Optimal control; Topological derivative; Turnpike phenomenon.

2020 Mathematics Subject Classification. 74P15, 49Q10, 35B25.

1. Introduction and Motivation

Gas transport through pipeline networks is a key part of the energy infrastructure, especially with hydrogen expected to become an important energy carrier in the near future. At the same time, natural gas is still widely used in households and industry across Europe. Pipelines are

E-mail address: michi.schuster@fau.de (M. Schuster), jan.sokolowski@univ-lorraine.fr (J. Sokolowski). Received 4 August 2025; Accepted 14 September 2025; Published online 24 November 2025.

^{*}Corresponding author.

a cost-efficient way to move gas over long distances, but the flow experiences a significant pressure drop due to friction along the pipeline. In fact, the *International Energy Outlook* 2018 [1] predicts that natural gas consumption will double until 2040 compared to 2012. For hydrogen transport, a new pipeline network is planned in Germany [2] and Europe [3]. In this paper we are interested in the optimal shape and control of gas transportation networks. The network is governed by the isothermal Euler equations [4, 5, 6, 7], a system of nonlinear hyperbolic PDEs. In [8], the authors discussed coupling conditions at the network junctions. In [9, 10], the authors gave an excellent overview about the broad topic of gas network modeling including model simplifications and network components. Optimization problems for electricity transport were analyzed e.g., in [11, 12], for traffic flow networks e.g., in [13, 14] and for communication and information networks e.g., in [15, 16].

We consider a dynamic optimal boundary control problem for the gas network. However, the optimum design problems for dynamic models are complex and we are interested in possible simplification for practical applications. To this end, for the further optimization with respect to the shape and topology of the gas network, it is proposed to use the optimal value of control cost in order to determine the optimum design solution for the network. The turnpike property of the optimal control problem is exploited to reduce the dynamic model to the static model for the purposes of shape and topology optimization. It means that the steady state model of the network as well as the associated optimal control problem are considered for the optimum design of network. Steady states models for gas networks were analyzed, e.g., in [17, 18, 19, 20].

In our setting, the shape functional for the networks is defined by the optimal value of the control cost for the associated steady state control problem. The proposed strategy is constructive because the topological derivatives of the shape functional are effectively determined for singular perturbations of the network. By the singular perturbation we mean the creation of a small cycle at the internal node of the network. The topological derivatives of shape functionals are introduced in [21] for singular geometrical domain perturbations in the shape optimization problems governed by partial differential equations of elliptic type. The concept of topological derivatives is also used for networks governed by linear PDEs in [22]. In shape and topology optimization there are two techniques used for numerical methods. The first is the shape sensitivity analysis with boundary variations for the geometrical domains. The second uses singular geometrical domain perturbations and leads to the topological derivatives. The geometrical domain is usually associated with the state equation. Similar methods can be applied on networks. Here, the singular perturbation of the network is the introduction of a small cycle at the network junctions. Our strategy is effecient and can be described as follows.

- (1) Let us consider the optimal control problem for gas networks. We determine the optimality conditions in the form of an optimality system. The optimal value of the cost is considered for optimum design of the network.
- (2) The turnpike property is checked for the control problem. This way the dynamic model is replaced by static model for the purposes of optimum design of the network.
- (3) The static control problem is considered and solved and the optimal value of the control cost is used as the shape functional for optimum design of the network.
- (4) The topological derivatives of the shape functional are evaluated for internal nodes of the network. The subset of the nodes with negative values of the topological derivatives

is selected for further topology changes by replacing the nodes with a small cycle. In this way the optimal network is constructed without further possibilities to change the topology in this way.

Concerning control of networks, the new concept for control problems is the *turnpike property*. The presence of such a property simplifies the analysis of control system because the evolution problem solution for large time horizon can be replaced by a combination of exact controllability for evolution model with the control of steady state model. We restrict ourselves to the simple model problems for the network with the tree structure. The turnpike property was analyzed in [23, 24] for the finite-dimensional setting and in [25] for the infinite-dimensional setting. Boundary control problems for linear hyperbolic PDEs were analyzed, e.g., in [26, 27]. Turnpike results based on dissipativity were analyzed in [28, 29], a manifold turnpike result was provided in [30]. The monograph [31] gives an excellent overview about the topic and in [32] the authors provide an excellent overview about further turnpike properties in finite and infinite dimensional optimal control. For semi-linear hyperbolic boundary control problems, to our best knowledge, turnpike properties have not been shown yet. We provide some numerical evidence of the turnpike property, however, the general semi-linear and nonlinear case is still an open problem.

The outline of the paper is the following. In *Section 2*, the turnpike property for semi-linear gas network control is considered from a numerical point of view. We provide numerical evidence for the turnpike phenomenon for an optimal boundary control problem governed by the isothermal Euler equations for both a single pipe and a network. In *Section 3*, the elementary junction as a subset of network is considered for the purposes of shape and topology optimization. We first derive the explicit solution on the network junction with and without a cycle. We analyze the optimal control problem for the network. For the optimal control, we compute the topological derivative and analyze the optimal design problem for the network junction. In *Section 4*, we present an algorithm based on the previous results for finding the optimal network topology. For every internal node in the network, we solve the optimal control problem and compute the topological derivative with respect to the optimal control. We replace the node with the smallest topological derivative by a small cycle and successively repeat this procedure until all topological derivatives are positive or until every internal node was replaced by a small cycle. To our best knowledge, this is the first work which combines optimal shape and control techniques for gas networks.

2. A Numerical Turnpike Result for the Gas Dynamics

The gas flow in a pipeline is modeled by the well-known isothermal Euler equations [4, 5, 6, 7] which consist in a 2×2 system of partial differential equations given by

$$\left\{egin{aligned} &
ho_t+q_x=0,\ &q_t+ig(p+
ho v^2ig)_x=-rac{\lambda}{2\,D}\,rac{q|q|}{
ho}, \end{aligned}
ight.$$

where $\rho = \rho(t,x)$ is the gas density in kg/m^3 , q = q(t,x) is the gas flow in kg/m^2s , p = p(t,x) is the gas pressure in Pa, v = v(t,x) is the gas velocity in m/s, $\lambda > 0$ is the pipe friction coefficient (no unit), D > 0 is the pipe diameter in m and $(t,x) \in [0,T] \times [0,L]$. Considering ideal gas, the

relation

$$p = c^2 \rho$$
,

holds, where c is the speed of sound in the gas in m/s. Excluding c^2 from the space derivative in the second equation leads to the space derivative

$$c^2\left(\rho+\rho\frac{v^2}{c^2}\right)_x$$

where v/c is the *Mach number*. For the gas flow in pipeline networks, the Mach number is close to 0, thus this term is often neglected (see, e.g., [33]), leading to a well-known semilinear model for the gas transport in a pipeline

$$\begin{cases}
 p_t + c^2 q_x = 0, \\
 q_t + p_x = -\frac{\lambda}{2} \frac{c^2}{D} \frac{q|q|}{p},
\end{cases} (2.1)$$

For initial conditions

$$p(0,x) = p_{\text{ini}}(x) \in L^2(0,L), \quad q(0,x) = q_{\text{ini}}(x) \in L^2(0,L),$$
 (2.2)

for boundary conditions

$$p(t,0) = p_0(t) \in L^2(0,T), \quad q(t,L) = q_L(t) \in L^2(0,T),$$

and if compatibility between initial and boundary conditions is satisfied, equations (2.1) have a solution $p,q \in C([0,T];L^2(0,L))$ (see e.g., [5]). Note that, for higher regularity, the solution has better regularity properties as well. Let initial conditions $p_{\text{ini}}, q_{\text{ini}} \in L^2(0,L)$ and convex functions $f,g:\mathbb{R}^2 \to \mathbb{R}$ be given. Consider the optimal control problem

$$\begin{split} \min_{p_0,q_L \in H^2(0,T)} & \int_0^T f(p_0(t),p(t,L)) + g(q(t,0),q_L(t)) \; dt, \\ \text{s.t.} & p(0,x) = p_{\text{ini}}(x), \; q(0,x) = q_{\text{ini}}(x), \\ & p_t + c^2 q_x = 0, \\ & q_t + p_x = -\frac{\lambda}{2} \frac{c^2}{D} \frac{q|q|}{p}, \\ & p(t,0) = p_0(t), \; q(t,L) = q_L(t). \end{split} \tag{2.3}$$

The existence of solutions of optimal control problems like (2.3) was analyzed on graphs recently (see [34]). The authors demonstrated that under the assumptions that the initial state is C^1 - compatible with the nodal conditions and that the control cost contains an H^2 -regularization term, an optimal control of (2.3) exists on networks. For a desired pressure $p_D \in \mathbb{R}^2$ and a desired flow $q_D \in \mathbb{R}^2$, let the objective function be given by

$$f(p_0(t), p(t, L)) = \left\| \begin{bmatrix} p_0(t) \\ p(t, L) \end{bmatrix} - p_D \right\|^2 = (p_0(t) - p_{D,1})^2 + (p(t, L) - p_{D,2})^2,$$
and
$$g(q(t, 0), q_L(t)) = \left\| \begin{bmatrix} q(t, 0) \\ q_L(t) \end{bmatrix} - q_D \right\|^2 = (q(t, 0) - q_{D,1})^2 + (q_L(t) - q_{D,2})^2.$$

As initial condition, we consider the steady state of (2.1) corresponding to the boundary conditions $p_0 = 50bar$ and $q_L = 180 \frac{kg}{m^2s}$. The optimal solution of (2.3) is shown in *Figure 1* and

it was computed using the *AMPL* software tool with the *ipopt* solver (see e.g., [35]) using 201 grid points for time discretization and 21 grid points for space discretization. The picture was created in *MATLAB*[®] *R2023b*. A turnpike structure is clearly visible, as the solution of (2.3), i.e., the dynamic optimal controls are close to the corresponding steady state optimal controls in the interior of the time interval. Only at the beginning and at the end of the time interval, dynamic and steady state optimal control differ.

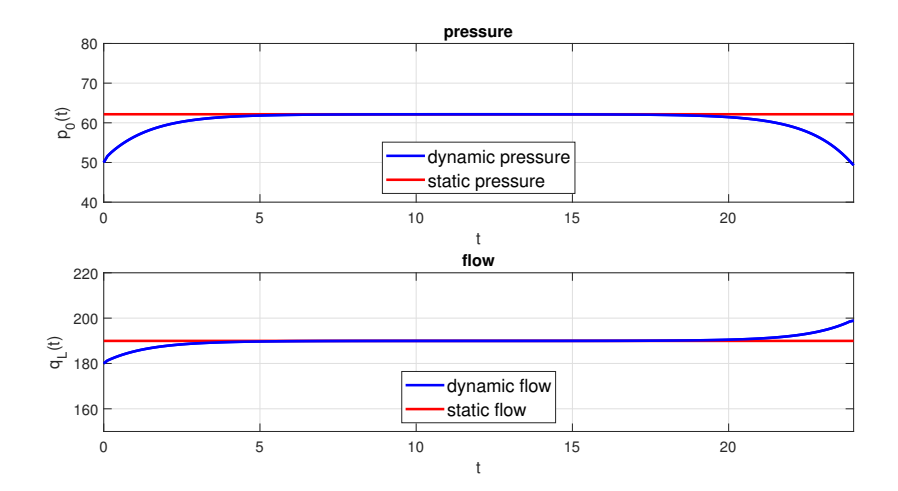


FIGURE 1. Result of (2.3) for T = 24h, L = 10km, $\lambda = 0.1$, c = 380m/s, D = 0.5m, $p_D = (60,55)^{\top} bar$ and $q_D = (180,200)^T \frac{kg}{m^2s}$.

This turnpike structure also occurs when coupling the model (2.1) on networks. We consider a network junction as shown in *Figure 2*. The gas model (2.1) and the initial conditions (2.2) hold on every edge. For the reader's convenience we consider equal pipe length, pipe diameter and pipe friction for every edge. The coupling conditions at the network junction are given by the conservation of mass

$$q_1(t,L) = q_2(t,0) + q_3(t,0) \qquad \forall t \in [0,T],$$
 (2.4)

and by the continuity in pressure

$$p_1(t,L) = p_2(t,0), \quad p_1(t,L) = p_3(t,0) \qquad \forall t \in [0,T].$$
 (2.5)

For boundary conditions

$$p_1(t,0) = p_0(t), \ q_2(t,L) = q_L(t), \ q_3(t,L) = \bar{q}_L(t),$$
 (2.6)

in $L^2(0,T)$, the gas model (2.1) with initial conditions (2.2) in $L^2(0,L)$ and coupling conditions (2.4), (2.5) has a solution $p_i, q_i \in C([0,T], L^2(0,L))$ [5]. Again, for higher regularity properties of the boundary conditions, the solution has better regularity properties as well.

Let initial conditions $p_{i,\text{ini}}, q_{i,\text{ini}}$ be given on every edge. For convex functions $f, g : \mathbb{R}^3 \to \mathbb{R}$ we consider the optimal control problem

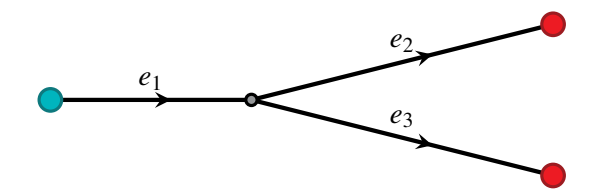


FIGURE 2. Gas Network Junction

$$\min_{p_0,q_L,\bar{q_L}\in L^2(0,T)} \quad \int_0^T f\left(p_0(t),p_2(t,L),p_3(t,L)\right) + g\left(q_1(t,0),q_L(t),\bar{q}(t)\right) \, dt,$$
 s.t.
$$p_i(0,x) = p_{i,\text{ini}}(x), \ q_i(0,x) = q_{i,\text{ini}}(x), \qquad \qquad i = 1,2,3$$

$$(p_i)_t + c^2(q_i)_x = 0, \qquad \qquad i = 1,2,3,$$

$$(q_i)_t + (p_i)_x = -\frac{\lambda}{2} \frac{c^2}{D} \frac{q_i|q_i|}{p_i}, \qquad \qquad i = 1,2,3,$$

$$p_1(t,0) = p_0(t), \ q_2(t,L) = q_L(t), \ q_3(t,L) = \bar{q}_L(t),$$

$$p_1(t,L) = p_2(t,0) = p_3(t,0), \ q_1(t,L) = q_2(t,0) + q_3(t,0).$$

$$(2.7)$$

As it was the case for the optimal control problem (2.3), the network model also shows a turnpike structure. For a desired pressure $p_D \in \mathbb{R}^3$ and a desired flow $q_D \in \mathbb{R}^3$, let the objective function be given by

$$f(p_0(t), p_1(t, L), p_2(t, L)) = \left\| \begin{bmatrix} p_0(t) \\ p_1(t, L) \\ p_2(t, L) \end{bmatrix} - p_D \right\|^2,$$

$$g(q_1(t, 0), q_L(t), \bar{q}_L(t)) = \left\| \begin{bmatrix} q_1(t, 0) \\ q_L(t) \\ \bar{q}_L(t) \end{bmatrix} - p_D \right\|^2.$$

As an initial condition, we consider the steady state of the network model corresponding to the boundary conditions $p_0 = 50bar$, $q_L = 100\frac{kg}{m^2s}$, and $\bar{q}_L = 80\frac{kg}{m^2s}$. As in the previous example, we use 201 grid points for time discretization and 21 grid points for space discretization on every edge. The optimal controls of (2.7) are shown in *Figure 3*. As above, the optimal controls of (2.7) are close to the corresponding steady state optimal controls in the interior of the time interval. They differ just at the beginning and at the end of the time interval. The corresponding pressure profiles at different time points are shown in *Figure 4*. The pressure profiles at the beginning and at the end of the time interval differ from the optimal steady state pressure profiles, while they are close to each other in the middle of the time interval, which supports the presence of the turnpike phenomenon. Thus, from now on, we assume that the optimal controls satisfy a turnpike inequality:

Assumption 2.1. The optimal control problems (2.3) and (2.7) satisfy an integral turnpike property of the form

$$\int_0^T \left\| u^{\delta}(t) - u^{\sigma} \right\|^2 dt \le C,$$

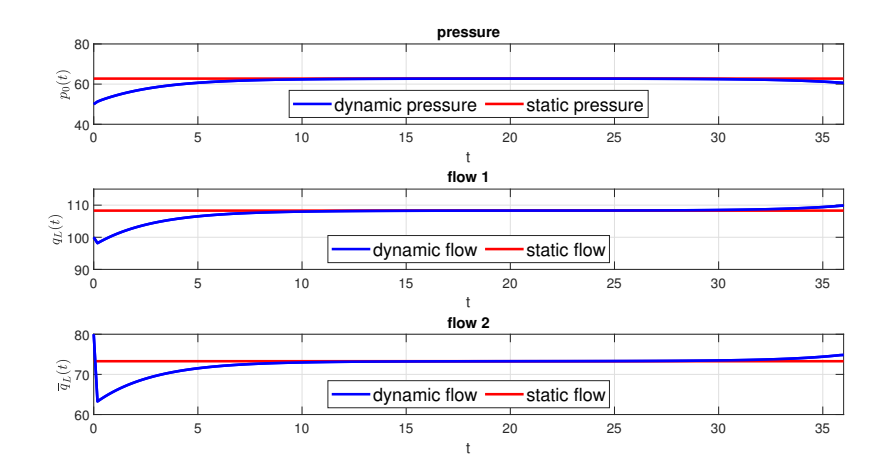


FIGURE 3. Result of (2.7) for T = 36h, L = 10km, $\lambda = 0.1$, c = 380m/s, D = 0.5m, $p_D = (60, 52, 55)bar$ and $q_D = (180, 110, 75) \frac{kg}{m^2s}$.

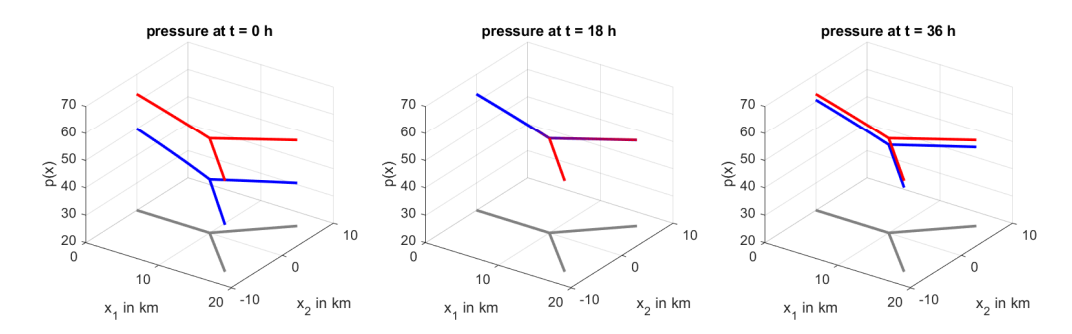


FIGURE 4. Pressure profiles of the solution of (2.7) at t = 0h, t = 18h and t = 36h.

where $u^{\delta}(t)$ is the solution of (2.3) resp. (2.7), u^{σ} is the solution of the corresponding steady state optimal control problems and $C \in \mathbb{R}$ is a time-independent constant.

In the next sections, we analyze the problem of optimal network topology, i.e., we analyze, if a network is more effective and beneficial when replaced by a cycle. Since operation of gas networks is planned for several hours, and due to the presence of a turnpike property, we consider steady states on gas networks, as they are often used to replace the transient models (see, e.g., [17, 19, 20, 36, 37]). Thus, in the next sections, we consider the problem of finding the optimal topology for junctions in gas networks for steady states.

3. Optimal Design and Shape for a Steady State Network Junction

In this section, we consider the problem of finding the optimal shape of a network junction in terms of gas flow in pipeline networks. Therefore, under the *Assumption 2.1*, we introduce a steady state model for the gas flow in pipeline networks, we compute the analytical solution for the flow on a network junction and we solve an optimal shape design problem for the network junction.

3.1. A steady state gas transport model on a network junction. Consider a connected directed graph $G = (\mathcal{V}, \mathcal{E})$ with a set of vertices \mathcal{V} with $|\mathcal{V}| = n$ and a set of edges $\mathcal{E} \subseteq \mathcal{V} \times \mathcal{V}$

with $|\mathscr{E}| = m$. Every edge e represents a pipe with length L^e . On every edge $e \in \mathscr{E}$, the gas flow is given by the steady state formulation of the semilinear isothermal Euler equations (2.1), i.e., on every edge $e \in \mathscr{E}$ we have (see, e.g., [17, 18, 19, 38])

$$\begin{cases} q_x^e(x) = 0, \\ p_x^e(x) = -\frac{\lambda^e}{2D^e} \frac{q^e(x)|q^e(x)|}{\rho^e(x)}, \end{cases}$$
(3.1)

where p is the gas pressure, ρ is the gas density, q is the gas flow, and λ is the pipe friction and D is the pipe diameter. The exponent e refers to edge $e \in \mathcal{E}$, respectively. The first equation in (3.1) implies constant flow on every edge. Thus, let $q \in \mathbb{R}^m$ be the vector of flows at the edges with $q_i = q^{e_i}$. Applying the ideal gas equation $p = R_S T \rho$ with the specific gas constant R_S and the temperature T, the second equation in (3.1) is

$$p_x^e(x) = -\frac{\lambda^e R_S T}{2D^e} \frac{q^e |q^e|}{p^e(x)},$$

which has the solution

$$(p^e(x))^2 = p^2(0) - \phi^e q^e |q^e| x$$
 with $\phi^e = \frac{\lambda^e R_S T}{D}$. (3.2)

For the reader's convenience, we assume equal ϕ^e on every pipe. That is, we have $\phi = \phi^e$ for all $e \in \mathscr{E}$. Let $p \in \mathbb{R}^n$ be the vector of pressures at the nodes with $p_i = p^{v_i}$. For every node $v \in \mathscr{V}$, let $\mathscr{E}_-(v)$ denote the ingoing edges, i.e., the edges that end in v and let $\mathscr{E}_+(v)$ be the set of outgoing edges, i.e., the edges that start in v. Every node can either be a source node (gas enters the network) or an exit node (gas leaves the network or gas is conserved in the network). Let \mathscr{V}_S be the set of source nodes and let \mathscr{V}_E be the set of exit nodes with $\mathscr{V}_S \cup \mathscr{V}_E = \mathscr{V}$, $\mathscr{V}_S \cap \mathscr{V}_E = \emptyset$. Let $b \in \mathbb{R}^n$ with $b_i = b^{v_i}$ be the load vector, i.e., the vector of gas entering or leaving the network. We assume $b_i < 0$ if gas enters the network at node v_i and $b_i \geq 0$ if gas leaves the network at node v_i , i.e., $b_i < 0$ for $v_i \in \mathscr{V}_S$ and $b_i \geq 0$ for $v_i \in \mathscr{V}_E$. We define the incidence matrix $A \in \mathbb{R}^{n \times m}$ with

$$A_{i,j} = \begin{cases} -1 & \text{if } e_j \in \mathcal{E}_+(v_i) \\ 1 & \text{if } e_j \in \mathcal{E}_-(v_i) \\ 0 & \text{else} \end{cases}$$

We consider conservation of mass at every node, i.e.,

$$\sum_{e \in \mathscr{E}_{-}(v)} q^e = \sum_{e \in \mathscr{E}_{+}(v)} q^e + b^v \qquad \forall v \in \mathscr{V}.$$

Applying the incidence matrix A, conservation of mass is equivalent to

$$Aq = b. (3.3)$$

Further, we consider continuity of the pressure at the nodes, i.e., for all $v \in \mathcal{V}$,

$$p^{e}(L) = p^{f}(0)$$
 $\forall e \in \mathscr{E}_{-}(v), f \in \mathscr{E}_{+}(v).$

Thus, applying (3.2) and the incidence matrix A, the pressure at the nodes can be computed by evaluating (see, e.g., [18, 19])

$$A^{\top} p^2 = \Phi q |q| L, \tag{3.4}$$

where Φ is a diagonal matrix with the entries $\Phi_{i,i} = \phi_i$ defined in (3.2). The square and the right-hand side product in (3.4) have to be understood component by component. Let p_i be given for all $v_i \in \mathcal{V}_S$ and let b_i be given for all $v_i \in \mathcal{V}_E$. Then the system (3.3), (3.4) has a unique solution (see [17]).

In this section, we consider a network junction without cycle $G_1 = (\mathcal{V}_1, \mathcal{E}_1)$ and a network junction with cycle $G_2 = (\mathcal{V}_2, \mathcal{E}_2)$, where the edges in the cycle have length ε , as given in *Table 1* and shown in *Figure 5*. In both graphs, let v_0 be the only inflow node, v_2, v_3 be outflow nodes, and all other nodes be inner nodes.

set of vertices	set of edges	edge orientation
$\mathcal{V}_1 = \{v_0, v_1, v_2\}$	$\mathscr{E}_1 = \{e_1, e_2, e_3\}$	$e_1 = (v_0, v_1), e_2 = (v_1, v_2), e_3 = (v_1, v_3)$
$\mathscr{V}_2 = \{v_0, v_1, v_2, v_3, v_4, v_5\}$	$\mathscr{E}_2 = \{e_1, e_2, e_3, e_4, e_5, e_6\}$	$\begin{vmatrix} e_1 = (v_0, v_1), e_2 = (v_4, v_2), e_3 = (v_5, v_3), \\ e_4 = (v_1, v_4), e_5 = (v_1, v_5), e_6 = (v_4, v_5) \end{vmatrix}$

TABLE 1. Set of vertices and set of edges of the graphs G_1 and G_2

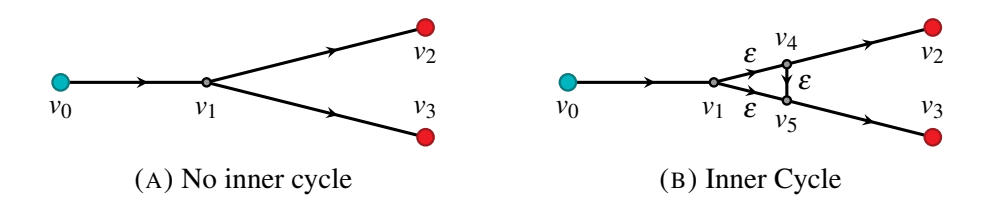


FIGURE 5. Network junction with and without inner cycle

In the following sections, we state the analytic solution for the pressure at the nodes and we consider the problem of finding the optimal size of the cycle, i.e. the optimal ε with respect to a suitable cost function.

3.2. Analytical solution for a junction without cycle. Let $p_0 > 0$, $b_1 = 0$ and $b_2, b_3 > 0$ be given. The incidence matrix A for the graph G_1 shown in Figure 5 (A) is given by

$$A = \begin{bmatrix} -1 & 0 & 0 \\ 1 & -1 & -1 \\ 0 & 1 & 0 \\ 0 & 0 & 1 \end{bmatrix}.$$

Thus, the conservation of mass (3.3) yields

$$q = [b_2 + b_3, b_2, b_3]^{\top}$$
 and $b = [-b_2 - b_3, 0, b_2, b_3]^{\top}$.

For the pressures at the nodes, the pressure continuity (3.4) yields

$$-p_0^2 + p_1^2 = -\phi q_1 |q_1| L_1,$$

$$-p_1^2 + p_2^2 = -\phi q_2 |q_2| L_2,$$

$$-p_1^2 + p_3^2 = -\phi q_3 |q_3| L_3.$$

Since $b_2, b_3 \ge 0$, we have $q \ge 0$ and we can neglect the absolute value. For $L_1 = L_2 = L_3 = \tilde{L}$, the pressure at the outflow nodes is given by

$$p_{2} = \sqrt{p_{0}^{2} - \phi q_{1}^{2} \tilde{L} - \phi q_{2}^{2} \tilde{L}} = \sqrt{p_{0}^{2} - \phi (q_{1}^{2} + q_{2}^{2}) \tilde{L}} = \sqrt{p_{0}^{2} + \phi (2b_{2}^{2} + 2b_{2}b_{3} + b_{3}^{2}) \tilde{L}},$$

$$p_{3} = \sqrt{p_{0}^{2} - \phi q_{1}^{2} \tilde{L} - \phi q_{3}^{2} \tilde{L}} = \sqrt{p_{0}^{2} - \phi (q_{1}^{2} + q_{3}^{2}) \tilde{L}} = \sqrt{p_{0}^{2} + \phi (b_{2}^{2} + 2b_{2}b_{3} + 2b_{3}^{2}) \tilde{L}}.$$

$$(3.5)$$

3.3. Analytical solution for a junction with cycle. Let p_0 , b_2 and b_3 be given. With the incidence matrix A being given by

$$A = \begin{bmatrix} -1 & 0 & 0 & 0 & 0 & 0 \\ 1 & 0 & 0 & -1 & -1 & 0 \\ 0 & 1 & 0 & 0 & 0 & 0 \\ 0 & 0 & 1 & 0 & 0 & 0 \\ 0 & -1 & 0 & 1 & 0 & -1 \\ 0 & 0 & -1 & 0 & 1 & 1 \end{bmatrix},$$

the third and fourth equation of mass conservation (3.3) yields $q_2 = b_2$ and $q_3 = b_3$. Further, we have

$$q_1 = b_2 + b_3$$
 and $b_0 = -b_2 - b_3$,

which implies

$$q = [b_2 + b_3, b_2, b_3, q_4, q_5, q_6]^{\top}$$
 and $b = [-b_2 - b_3, 0, b_2, b_3, 0, 0]^{\top}$.

Before we compute the remaining flows q_4, q_5, q_6 , we state the following remark.

Remark 3.1. Cyclic flow in G_2 is not possible, since the pressure decreases along a pipe in flow direction. Consider, e.g., the cyclic flow $q_4 > 0$, $q_5 < 0$, $q_6 > 0$, which leads to the contradiction

$$p_1 < p_5 < p_4 < p_1$$

If flow q_4 is negative, then q_5 must be positive and q_6 negative to guarantee a positive flow q_2 . This would lead to a cyclic flow and thus to a contradiction. If flow q_5 is negative, then q_4 and q_6 must be positive to guarantee a positive flow q_3 . This would also lead to a contradiction due to a cyclic flow. Thus we have

$$q_4 > 0$$
 and $q_5 > 0$,

and we can neglect the absolute value for the pressure loss (3.2) for e_4 and e_5 .

Without loss of generality, we assume $b_3 \ge b_2$, which implies

$$q_6 \ge 0 \tag{3.6}$$

because otherwise we have $q_5 > q_4$. Thus the pressure loss from v_1 to v_4 via e_5 and e_6 is larger than the pressure loss from v_1 to v_4 via e_4 . Consequently, we can also neglect the absolute value for the pressure loss (3.2) for e_6 .

Given $q_1 = b_2 + b_3$, $q_2 = b_2$ and $q_3 = b_3$, conservation of mass (3.3) yields

$$-q_4 - q_5 = -b_2 - b_3 (3.7a)$$

$$q_4 - q_6 = b_2 (3.7b)$$

$$q_5 + q_6 = b_3 (3.7c)$$

Continuity in pressure (3.4) yields

$$p_1^2 - p_4^2 = \phi q_4^2 \varepsilon \tag{3.8a}$$

$$p_1^2 - p_5^2 = \phi q_5^2 \varepsilon \tag{3.8b}$$

$$p_4^2 - p_5^2 = \phi q_6^2 \varepsilon \tag{3.8c}$$

Adding (3.8a) and (3.8c) leads to

$$p_1^2 - p_5^2 = \phi(q_4^2 + q_6^2)\varepsilon \stackrel{\text{(3.8b)}}{=} \phi q_5^2 \varepsilon \iff q_4^2 - q_5^2 + q_6^2 = 0$$
 (3.9)

Inserting (3.7b) and (3.7c) into (3.9) implies

$$(b_2+q_6)^2-(b_3-q_6)^2+q_6^2=0 \iff q_6^2+2(b_2+b_3)q_6+b_2^2-b_3^2=0.$$

Solving the quadratic equation, we have

$$q_6 = \frac{1}{2} \left[-2(b_2 + b_3) \pm \sqrt{4(b_2 + b_3)^2 - 4(b_2^2 - b_3^2)} \right]$$

$$= \frac{1}{2} \left[-2(b_2 + b_3) \pm \sqrt{8b_2b_3 + 2b_3^2} \right]$$

$$= \frac{1}{2} \left[-2\sqrt{b_2^2 + 2b_2b_3 + b_3^2} \pm 2\sqrt{b_3^2 + 2b_2b_3 + b_3^2} \right]$$

Since $b_2, b_3 > 0$, both solutions for q_6 exist, but the negative branch of the solution yields $q_6 < 0$, which is a contradiction to (3.6). Thus

$$q_6 = \sqrt{2}\sqrt{b_2b_3 + b_3^2} - b_2 - b_3 \stackrel{b_3 \ge b_2}{\ge} 0,$$

is the unique solution of q_6 . Note that $q_6 = 0$ for $b_3 = b_2$ and $q_6 > 0$ for $b_3 > b_2$. With (3.7b), we have

$$q_4 = \sqrt{2}\sqrt{b_2b_3 + b_3^2} - b_3 \stackrel{b_3 \ge b_2}{\ge} 0,$$

and with (3.7c) we have

$$q_5 = b_2 + 2b_3 - \sqrt{2}\sqrt{b_2b_3 + b_3^2} \stackrel{b_3 \ge b_2}{\ge} 0.$$

For pipe lengths $L_1 = \tilde{L}$, $L_2 = L_3 = \tilde{L} - \varepsilon$ and $L_4 = L_5 = L_6 = \varepsilon$, the pressure at the nodes is given by

$$\begin{split} p_1 &= \sqrt{p_0^2 - \phi q_1^2 \tilde{L}}, \\ p_4 &= \sqrt{p_1^2 - \phi q_4^2 \varepsilon} = \sqrt{p_0^2 - \phi q_1^2 \tilde{L} - \phi q_4^2 \varepsilon}, \\ p_5 &= \sqrt{p_1^2 - \phi q_5^2 \varepsilon} = \sqrt{p_0^2 - \phi q_1^2 \tilde{L} - \phi q_5^2 \varepsilon}, \\ p_2 &= \sqrt{p_4^2 - \phi q_2^2 (\tilde{L} - \varepsilon)} = \sqrt{p_0^2 - \phi (q_1^2 + q_2^2) \tilde{L} - \phi (q_4^2 - q_2^2) \varepsilon}, \\ p_3 &= \sqrt{p_5^2 - \phi q_3^2 (\tilde{L} - \varepsilon)} = \sqrt{p_0^2 - \phi (q_1^2 + q_3^2) \tilde{L} - \phi (q_5^2 - q_3^2) \varepsilon}. \end{split}$$

Inserting the flows implies

$$p_{2} = \sqrt{p_{0}^{2} - \phi \left(2b_{2}^{2} + 2b_{2}b_{3} + b_{3}^{2}\right)\tilde{L} - \phi \left(-b_{2}^{2} + 2b_{2}b_{3} + 3b_{3}^{2} - 2\sqrt{2}b_{3}\sqrt{b_{2}b_{3} + b_{3}^{2}}\right)\varepsilon},$$

$$p_{3} = \sqrt{p_{0}^{2} - \phi \left(b_{2}^{2} + 2b_{2}b_{3} + 2b_{3}^{2}\right)\tilde{L} - \phi \left(b_{2}^{2} + 6b_{2}b_{3} + 5b_{3}^{2} - 2\sqrt{2}(b_{2} + 2b_{3})\sqrt{b_{2}b_{3} + b_{3}^{2}}\right)\varepsilon}.$$

For

$$k_{2,1} := 2b_2^2 + 2b_2b_3 + b_3^2,$$
 $k_{2,2} := -b_2^2 + 2b_2b_3 + 3b_3^2 - 2\sqrt{2}b_3\sqrt{b_2b_3 + b_3^2},$ $k_{3,1} := b_2^2 + 2b_2b_3 + 2b_3^2,$ $k_{3,2} := b_2^2 + 6b_2b_3 + 5b_3^2 - 2\sqrt{2}(b_2 + 2b_3)\sqrt{b_2b_3 + b_3^2},$

we have

$$p_2 = \sqrt{p_0^2 - \phi k_{2,1} \tilde{L} - \phi k_{2,2} \varepsilon}, \qquad p_3 = \sqrt{p_0^2 - \phi k_{3,1} \tilde{L} - \phi k_{3,2} \varepsilon}.$$
 (3.10)

Remark 3.2. Note that the pressures stated in (3.10) coincide with the pressures stated in (3.5) for $\varepsilon = 0$.

Remark 3.3. For $b_2 > b_3$, we have $q_6 \le 0$ and the pressures are given by

$$p_{2} = \sqrt{p_{0}^{2} - \phi \left(2b_{2}^{2} + 2b_{2}b_{3} + b_{3}^{2}\right)\tilde{L} - \phi \left(5b_{2}^{2} + 6b_{2}b_{3} + b_{3}^{2} - 2\sqrt{2}(2b_{2} + b_{3})\sqrt{b_{2}^{2} + b_{2}b_{3}}\right)\varepsilon},$$

$$p_{3} = \sqrt{p_{0}^{2} - \phi \left(b_{2}^{2} + 2b_{2}b_{3} + 2b_{3}^{2}\right)\tilde{L} - \phi \left(3b_{2}^{2} + 2b_{2}b_{3} - b_{3}^{2} - 2\sqrt{2}b_{2}\sqrt{b_{2}^{2} + b_{2}b_{3}}\right)\varepsilon}}$$
(3.11)

3.4. The optimal design problem. Consider a continuously differentiable function

$$f: \mathbb{R} \to \mathbb{R}, \qquad f: \varepsilon \mapsto \omega_2(p_2(\varepsilon) - \bar{p})^2 + \omega_3(p_3(\varepsilon) - \bar{p})^2,$$

with weights $\omega_2, \omega_3 > 0$ and a reference pressure $\bar{p} \in \mathbb{R}_{\geq 0}$. Often, in applications, the pressure needs to satisfy box constraints $[p_{\min}, p_{\max}]$ such that \bar{p} can be chosen as $(p_{\min} + p_{\max})/2$. We consider the optimal shape problem

$$\min_{\varepsilon \in \mathbb{R}} \quad f(\varepsilon), \qquad \text{s.t.} \quad \varepsilon \ge 0. \tag{3.12}$$

Assume that p_0 is sufficiently large such that $p_2, p_3 \ge 0$. Since ε is bounded from below by 0 and from above by \tilde{L} , due to the continuity of f, optimal design problem (3.12) has at least one solution by the *extreme value theorem*. We now compute the topological derivative

$$\mathscr{T}(v_1) = \lim_{\varepsilon \searrow 0^+} \frac{f(\varepsilon) - f(0)}{\varepsilon} = f'(0^+).$$

If the topological derivative $\mathcal{T}(v_1)$ is non-negative, then the network without cycle *Figure 5 (A)* provides a lower objective value than the objective value for the network *Figure 5 (B)* for any $\varepsilon > 0$. We have

$$f'(\varepsilon) = 2\omega_2(p_2(\varepsilon) - \bar{p}) \cdot p_2'(\varepsilon) + 2\omega_3(p_3(\varepsilon) - \bar{p}) \cdot p_3'(\varepsilon).$$

For the derivative of p_2 and p_3 , we obtain

$$p_2'(\varepsilon) = \frac{1}{2} \frac{1}{p_2(\varepsilon)} \Big(-\phi k_{2,2} \Big), \qquad p_3'(\varepsilon) = \frac{1}{2} \frac{1}{p_3(\varepsilon)} \Big(-\phi k_{3,2} \Big),$$

which implies

$$f'(\varepsilon) = -\omega_2(p_2(\varepsilon) - \bar{p}) \cdot \frac{\phi k_{2,2}}{p_2(\varepsilon)} - \omega_3(p_3(\varepsilon) - \bar{p}) \cdot \frac{\phi k_{3,2}}{p_3(\varepsilon)}.$$

Thus

$$\mathcal{T}(v_{1}) = -\omega_{2}(p_{2}(0^{+}) - \bar{p}) \cdot \frac{k_{2}}{p_{2}(0^{+})} - \omega_{3}(p_{3}(0^{+}) - \bar{p}) \cdot \frac{k_{3}}{p_{3}(0^{+})}
= -\omega_{2} \frac{k_{2,2} \left(\sqrt{p_{0}^{2} - \phi k_{2,1}\tilde{L}} - \bar{p}\right)}{\sqrt{p_{0}^{2} - \phi k_{2,1}\tilde{L}}} - \omega_{3} \frac{k_{3} \left(\sqrt{p_{0}^{2} - \phi k_{3,1}\tilde{L}} - \bar{p}\right)}{\sqrt{p_{0}^{2} - \phi k_{3,1}\tilde{L}}}.$$
(3.13)

Note that, for $b_2 = b_3$ we have $k_2 = k_3 = 0$, i.e., for symmetric outflow, for every $\varepsilon \in (0, \tilde{L}]$, we have $q_6 = 0$. Thus the topological derivative does not provide any insights, since the cycle is not used for gas transport. For $b_3 > b_2$, we have $k_3 < 0 < k_2$, since some gas on its way from v_0 to v_3 passes v_1, v_4 and v_5 , and thus the pressure loss between v_1 and v_2 is higher compared to the junction without cycle. So, for $b_2 \neq b_3$, one term in the topological derivative (3.13) is always positive, one term is always negative and the sign of (3.13) strongly depends on the weights ω_2, ω_3 and on the reference pressure \bar{p} . In *Figure* 6, we present an example with the optimal values for ε for different reference pressures \bar{p} . In *Figure* 6 (A), we have $\mathcal{T}(v_1) > 0$, while, in *Figure* 6 (B) and (C), we have $\mathcal{T}(v_1) < 0$.

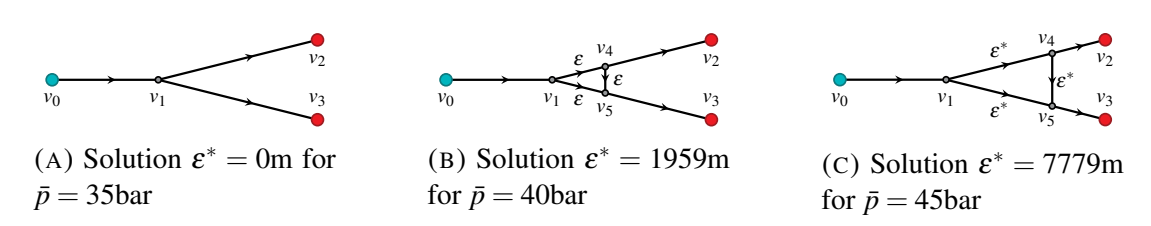


FIGURE 6. Optimal shape of a network junction for different reference pressures with weights $\omega_2 = \omega_3 = 1$, pipe length $\tilde{L} = 1 \cdot 10^4$ m, constant $\phi = 14714$ m/s² and outflows $b_2 = 120$ kg/m²s, $b_3 = 150$ kg/m²s.

For $b_3 \ge b_2$ we have $p_3 \le p_2$ and we can also observe that the smallest pressure in the network p_3 increases with increasing ε , allowing smaller inlet pressures p_0 . Thus it is natural to consider an objective function depending on p_0 , p_2 and p_3 , as we do in the next section.

3.5. The optimal design and control problem. In this section, we consider the optimal design and control problem for a network junction, where the control is the initial pressure at node v_0 . Consider the continuously differentiable function

$$f: \mathbb{R}^2 \to \mathbb{R}, \quad f: (p_0, \varepsilon) \mapsto \omega_0(p_0 - \bar{p}_0)^2 + \omega_2(p_2(p_0, \varepsilon) - \bar{p})^2 + \omega_3(p_3(p_0, \varepsilon) - \bar{p})^2,$$

with weights $\omega_0, \omega_2, \omega_3 > 0$ and reference pressures $\bar{p}_0, \bar{p} \in \mathbb{R}_{\geq 0}$. Consider the optimal design and control problem

$$\min_{(p_0,\varepsilon)} f(p_0,\varepsilon) \quad \text{s.t.} \quad \varepsilon \ge 0, \ p_0 \ge 0$$
 (3.14)

In order to extend the results later to tree-structured networks, we first consider the problem of finding the minimal inlet pressure p_0 for given ε . For a given $0 \le \varepsilon \le \tilde{L}$, consider the optimal control problem

$$\min_{p_0 \in \mathbb{R}} \quad f(p_0, \varepsilon) \qquad \text{s.t.} \quad p_0 \ge 0 \tag{3.15}$$

Lemma 3.1. *The optimal control problem* (3.15) *has a unique solution.*

Proof. For $b_3 \geq b_2$, there exists a lower bound $\underline{p_0}$, s.t. $p_3 \notin \mathbb{R}$ for $p_0 < \underline{p_0}$. Further, since $\lim_{p_0 \to \infty} f(p_0, \varepsilon) = \infty$, we can find $\overline{p_0}$ with $f(p_0, \varepsilon) \geq f(\overline{p_0}, \varepsilon)$ for all $p_0 \geq \overline{p_0}$. Thus, a solution of (3.15) exists due to the *extreme value theorem*.

For the uniqueness, we show the strict convexity of $f(p_0, \varepsilon)$ w.r.t. p_0 . Note that

$$\frac{\partial}{\partial p_0} f(p_0, \varepsilon) = 2\omega_0(p_0 - \bar{p}_0) + 2\omega_2 \frac{(p_2(p_0, \varepsilon) - \bar{p})p_0}{p_2(p_0, \varepsilon)} + 2\omega_3 \frac{(p_3(p_0, \varepsilon) - \bar{p})p_0}{p_3(p_0, \varepsilon)}
= 2\omega_0(p_0 - \bar{p}_0) + 2\omega_2 \left[p_0 - \bar{p} \frac{p_0}{p_2(p_0, \varepsilon)} \right] + 2\omega_3 \left[p_0 - \bar{p} \frac{p_0}{p_3(p_0, \varepsilon)} \right].$$

For the second derivative we have

$$\frac{\partial^2}{\partial p_0^2} f(p_0, \varepsilon) = 2(\omega_0 + \omega_2 + \omega_3) - \bar{p} \left[\frac{p_2(p_0, \varepsilon) - p_0^2 p_2^{-1}(p_0, \varepsilon)}{p_2(p_0, \varepsilon)^2} \right] - \bar{p} \left[\frac{p_3(p_0, \varepsilon) - p_0^2 p_3^{-1}(p_0, \varepsilon)}{p_3(p_0, \varepsilon)^2} \right].$$

For $b_2, b_3 > 0$ we have $p_0 > p_2(p_0, \varepsilon), p_3(p_0, \varepsilon)$ and thus

$$p_0 p_j^{-1}(p_0, \varepsilon) > 1$$
 and $p_j(p_0, \varepsilon) - p_0^2 p_j^{-1}(p_0, \varepsilon) < 0$, $j \in \{2, 3\}$.

Consequently we have $\frac{\partial^2}{\partial p_0^2} f(p_0, \varepsilon) > 0$, which means f is strictly convex and for $0 < \varepsilon \le \tilde{L}$, the optimal control problem (3.15) has a unique solution.

Let $p_0^*(\varepsilon)$ be the unique optimal solution of (3.15) given by the stationary point of $f(p_0, \cdot)$, or, if the stationary point leads to complex pressures p_2, p_3 , by the smallest possible value for p_0 , such that p_2 and p_3 are real. We assume that \bar{p}_0 and \bar{p} are sufficiently large such that the stationary point of $f(p_0, \cdot)$ is always feasible. Then the unique optimal solution $p_0^*(\varepsilon)$ of (3.15) is given by the solution of

$$0 = \frac{\partial}{\partial p_0} f(p_0^*(\varepsilon), \varepsilon)$$

$$= 2\omega_0(p_0^*(\varepsilon) - \bar{p}_0) + 2\omega_2 \left[p_0^*(\varepsilon) - \bar{p} \frac{p_0^*(\varepsilon)}{p_2(p_0^*(\varepsilon), \varepsilon)} \right] + 2\omega_3 \left[p_0^*(\varepsilon) - \bar{p} \frac{p_0^*(\varepsilon)}{p_3(p_0^*(\varepsilon), \varepsilon)} \right]$$
(3.16)

The optimal cost corresponding to $p_0^*(\varepsilon)$ is given by

$$J(\varepsilon) := f(p_0^*(\varepsilon), \varepsilon).$$

Then, the topological derivative $\mathcal{T}_J(v_1)$ is given by

$$\mathscr{T}_{J}(v_{1}) = \lim_{\varepsilon \searrow 0^{+}} \frac{J(\varepsilon) - J(0)}{\varepsilon} = \lim_{\varepsilon \searrow 0^{+}} \frac{f(p_{0}^{*}(\varepsilon), \varepsilon) - f(p_{0}^{*}(0), 0)}{\varepsilon}, \tag{3.17}$$

which can be approximated by solving (3.16) for small $\varepsilon > 0$ and for $\varepsilon = 0$. If the topological derivative is non-negative, $J(\varepsilon)$ does not decrease if we add a cycle to the network. If the topological derivative is negative, a cycle in the network decreases the cost $J(\varepsilon)$.

Note that the problem of finding the optimal cycle size w.r.t. the optimal control (3.16) is equivalent to solving a bilevel optimization problem with the optimal cycle size on the upper level and the optimal control on the lower level. Applying (3.16) for the lower level, the optimal size of the cycle ε can be computed by solving the optimization problem

With the data from Figure 6 (B) and for $\omega_0 = 1$, $\bar{p}_0 = 60$, the topological derivative (3.17) is negative, which implies that a cycle decreases the control cost. The solution ε^* of (3.18) and its corresponding optimal control are given by

$$\varepsilon^* = 8824m$$
, $p_0^*(\varepsilon^*) = 55.49$ bar,

and the corresponding optimal pressures are given by

$$p_2(p_0^*(\varepsilon^*), \varepsilon^*) = 41.79$$
bar, $p_3(p_0^*(\varepsilon^*), \varepsilon^*) = 41.59$ bar.

4. TOPOLOGICAL DERIVATIVE METHOD FOR OPTIMAL DESIGN STRATEGY FOR STEADY STATE DISTRIBUTION NETWORKS

In this section, we provide a strategy for the optimal design of a gas distribution network based on the results of the last section. Consider a connected, directed, tree-structured graph $G = (\mathcal{V}, \mathcal{E})$ with a single source node, i.e., we have $|\mathcal{V}_S| = 1$ and $|\mathcal{E}_-(v)| \le 1$ for all $v \in \mathcal{V}$. Assume that all network junctions are of the form *Figure 5 (A)*, i.e., we have $|\mathcal{E}_+(v)| = 2$ for inner nodes (with $b^v = 0$) and $|\mathcal{E}_+(v)| = 0$ for exit nodes ($b^v > 0$). An example graph is shown in *Figure 7*. Let

$$\mathcal{V}_J := \{ v \in \mathcal{V} \mid |\mathcal{E}_+(v)| = 2 \},$$

be the set of network junctions.

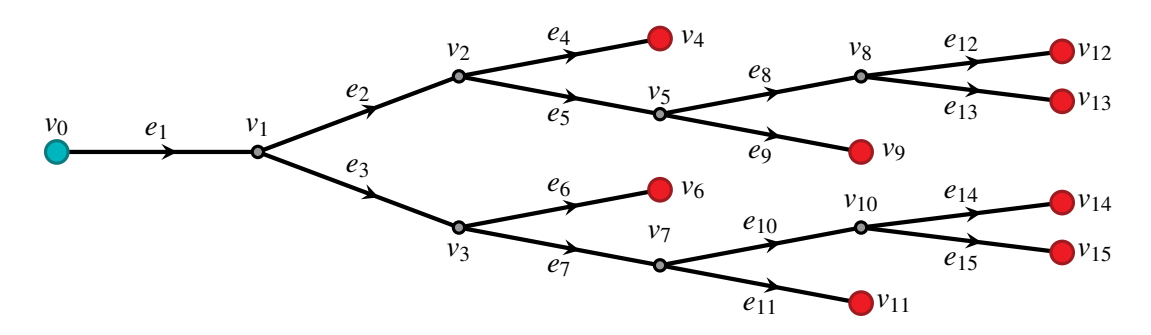


FIGURE 7. Tree-structured network graph with source node (blue), inner nodes (gray) and exit nodes (red)

Let the pressure given at the source node v_0 and let outflows b_i be given for all $v_i \in \mathcal{V}_E$ with $b_i = 0$ for all $v_i \in \mathcal{V}_J$. Then, the conservation of mass yields

$$b^{v_0} = \sum_{i=1}^n b^{v_i}.$$

Let \bar{A} be the incidence matrix without the first row (corresponding to v_0). Then \bar{A} is square and of full rank (see, e.g., [18]), thus the flow at the edges is given by mass conservation

$$q = \bar{A}^{-1}\bar{b},$$

i.e., the flow at the edges is a priori known. Instead of solving the optimal design and control problem (3.14) for the whole graph, which requires enormous effort for large graphs, we provide a strategy based on the problems (3.15), (3.18) and the topological derivative (3.17) to obtain an efficient network structure while keeping the control cost low. Therefore, we introduce the set \mathcal{V}_C of network junctions that contain a cycle (c.f., *Figure 5 (B)*), which is empty for now, but this will change when following the proposed algorithm. Further, for $j \in \mathcal{V}_J$, we define the continuously differentiable cost functions

$$f: \mathbb{R}^2 \to \mathbb{R}, \qquad f: (p_0, \varepsilon_j) \mapsto \omega_0(p_0 - \bar{p}_0)^2 + \sum_{i \in \mathscr{V}_F} \omega_i(p_i(p_0, \varepsilon_j) - \bar{p}_i)^2,$$

with weights $\omega_0, \omega_i > 0$ and reference pressures $\bar{p}_0, \bar{p}_i \in \mathbb{R}_{\geq 0}$, for all $i \in \mathcal{V}_E$. The cost function f_j refers to the graph G that has a cycle of variable length ε_j at node v_j . Note that for the readers' convenience we write $i \in \mathcal{V}_E$ and $j \in \mathcal{V}_J$ instead of $v_i \in \mathcal{V}_E$ and $v_j \in \mathcal{V}_J$ for the index of node v_i and v_j , respectively. The strategy to obtain an efficient network topology with low control cost is stated in the following algorithm:

The key idea of *Algorithm 1* is to successively add a cycle to the network junction, which is most beneficial with respect to the topological derivative of this junction. In the following, we will analyze *Algorithm 1* step by step.

Line 1-4: Instead of solving the optimal design and control problem (3.14), we consider a cycle at every network junction separately. Thus, in a loop we consider $|\mathcal{V}_{\mathcal{I}}|$ graphs with an additional cycle at a different location in each iteration.

Line 2: For every network junction $v_j \in \mathscr{V}_J$ we compute the optimal control $p_0^*(\varepsilon_j)$ (c.f., (3.15)), which exists due to *Lemma 3.1*. As it was mentioned before, the optimal control $p_0^*(\varepsilon_j)$ is either given by the stationary point of $\frac{\partial}{\partial p_0} f(p_0^*(\varepsilon_j), \varepsilon_j)$, if \bar{p}_0 and \bar{p}_i ($i \in \mathscr{V}_E$) are sufficiently large, or by the lowest possible pressure \underline{p}_0 , such that $p_i(p_0, \cdot)$ is real for all $i \in \mathscr{V}_E$. Thus we have

$$p_0^*(\varepsilon_j) = \begin{cases} \text{unique solution of } \frac{\partial}{\partial p_0} f(p_0^*(\varepsilon_j), \varepsilon_j) = 0 & \text{if } p_i(p_0^*(\cdot), \cdot) \text{ is real for all } \in \mathscr{V}_E \\ \underline{p}_0 & \text{else} \end{cases}$$

The derivative of f with respect to p_0 is given by (c.f., (3.16))

$$\frac{\partial}{\partial p_0} f(p_0(\varepsilon), \varepsilon) = 2\omega_0(p_0(\varepsilon) - \bar{p}_0) + \sum_{i \in \mathscr{V}_E} 2\omega_i \left[p_0(\varepsilon) - \bar{p}_i \frac{p_0(\varepsilon)}{p_i(p_0(\varepsilon), \varepsilon)} \right].$$

The pressures $p_i(p_0(\varepsilon_j), \varepsilon_j)$ can be evaluated following the path from v_0 to v_i ($i \in \mathscr{V}_E$). Note that since the graph is tree-structured, every network junction is either of the form *Figure 5 (A)* or *Figure 5 (B)* without the first edge, respectively. Thus, if v_k is on the path from v_0 to v_i with the two outgoing edges $e_\ell = (v_k, v_\ell)$ and $e_m = (v_k, v_m)$, we have

$$p_{\ell} = \sqrt{p_k^2 - \phi b_{\ell}^2 \tilde{L}}, \qquad p_m = \sqrt{p_k^2 - \phi b_m^2 \tilde{L}} \qquad \text{if } v_k \in \mathcal{V}_J \text{ (c.f., (3.5))},$$

Algorithm 1 Optimal Design Strategy for Tree-Structured Networks

- 1: **for each** $j \in \mathcal{V}_J$ **do**
- 2: Add a cycle of length $\varepsilon > 0$ to node v_i and solve the optimal control problem

$$\min_{p_0 \in \mathbb{R}} \quad f_j(p_0, \boldsymbol{\varepsilon}_j) \qquad ext{s.t.} \quad \boldsymbol{\varepsilon}_j \geq 0, \ p_0 \geq 0.$$

3: Define the optimal cost as

$$J_i(\varepsilon_i) = f_i(p_0^*(\varepsilon_i), \varepsilon_i),$$

compute the topological derivative

$$\mathscr{T}_{J_j}(v_j) = \lim_{\varepsilon_i \searrow 0^+} \frac{J_j(\varepsilon_j) - J_j(0)}{\varepsilon_j} = \lim_{\varepsilon_i \searrow 0^+} \frac{f_j(p_0^*(\varepsilon_j), \varepsilon_j) - f_j(p_0^*(0), 0)}{\varepsilon_j}.$$

- 4: end for
- 5: **if** $\mathscr{T}_{J_i}(v_j) \geq 0$ for all $j \in \mathscr{V}_J$ **then**
- 6: Stop
- 7: else
- 8: Set $j^* := \min_{i \in \mathcal{V}_I} \mathcal{T}_{J_i}(v_i)$
- 9: end if
- 10: Solve the optimal design problem

$$\varepsilon_{j^*}^* := \min_{\varepsilon \ge 0} J_{j^*}(\varepsilon_{j^*}) \quad \text{s.t.} \quad \frac{\partial}{\partial p_0} f_{j^*}(p_0^*(\varepsilon_{j^*}), \varepsilon_{j^*}) = 0. \tag{4.1}$$

Replace v_{j^*} by a cycle with length $\mathcal{E}_{j^*}^*$, remove v_{j^*} from \mathcal{V}_J and add v_{j^*} to \mathcal{V}_C .

- 11: **if** $\mathcal{V}_J = \emptyset$ **then**
- 12: Stop
- 13: **end if**
- 14: Return to 1.

i.e., if the network junction v_k does not contain a cycle, we have

$$p_{\ell} = \sqrt{p_{k}^{2} - \phi b_{\ell}^{2} \tilde{L} - \phi \left(-b_{\ell}^{2} + 2b_{\ell} b_{m} + 3b_{m}^{2} - 2\sqrt{2}b_{m} \sqrt{b_{\ell} b_{m} + b_{m}^{2}}\right) \varepsilon_{k}}$$
 if $v_{k} \in \mathscr{V}_{C}$ and $b_{m} \geq b_{\ell}$
$$p_{m} = \sqrt{p_{k}^{2} - \phi b_{m}^{2} \tilde{L} - \phi \left(b_{\ell}^{2} + 6b_{\ell} b_{m} + 5b_{m}^{2} - 2\sqrt{2}(b_{\ell} + 2b_{m})\sqrt{b_{\ell} b_{m} + b_{m}^{2}}\right) \varepsilon_{k}}$$
 (c.f., (3.10)).

and

$$p_{\ell} = \sqrt{p_{k}^{2} - \phi b_{\ell}^{2} \tilde{L} - \phi \left(5b_{\ell}^{2} + 6b_{\ell}b_{m} + b_{m}^{2} - 2\sqrt{2}(2b_{\ell} + b_{m})\sqrt{b_{\ell}^{2} + b_{\ell}b_{m}}\right)} \varepsilon_{k}}$$
 if $v_{k} \in \mathscr{V}_{C}$ and $b_{m} < b_{\ell}$
$$p_{m} = \sqrt{p_{k}^{2} - \phi b_{m}^{2} \tilde{L} - \phi \left(3b_{\ell}^{2} + 2b_{\ell}b_{m} - b_{m}^{2} - 2\sqrt{2}b_{\ell}\sqrt{b_{\ell}^{2} + b_{\ell}b_{m}}\right)} \varepsilon_{k}}$$
 (c.f., (3.11)).

Line 3: For every network junction $v_j \in \mathcal{V}_J$ with corresponding optimal control $p_0^*(\varepsilon_j)$ we compute the topological derivative $\mathcal{T}_{J_i}(v_j)$, which can be approximated by solving

$$\frac{\partial}{\partial p_0} f(p_0^*(\varepsilon_j), \varepsilon_j) = 0,$$

for small ε_j and for $\varepsilon_j = 0$. If the topological derivative is negative, adding a cycle decreases the cost $J_j(\varepsilon_j)$, if it is positive, a cycle does not provide any benefit.

Line 5-9: If all topological derivatives are non-negative, adding a cycle to any network junction does not provide any benefit, thus the algorithm has terminated and the resulting graph consists of the source node \mathcal{V}_S , the network junctions without cycle \mathcal{V}_J , the network junctions with a cycle \mathcal{V}_C and the exit nodes \mathcal{V}_E . If at least one topological derivative is negative, we save the index of the network junction with the smallest topological derivative as j^* , since adding a cycle to the network junction v_{j^*} provides the highest benefit.

Line 10: Since adding a cycle to v_{j^*} provides the highest benefit for the graph, we solve the optimal design problem (4.1) depending on the optimal inlet pressure $p_0^*(\varepsilon_{j^*})$. Thus, for the optimal solution $\varepsilon_{j^*}^*$ of (4.1), we add the cycle of length $\varepsilon_{j^*}^*$ to the network junction v_{j^*} . Since the junction now contains a cycle, we remove it from the set of network junctions without cycles \mathcal{V}_J and add it to the set of network junctions with cycles \mathcal{V}_C .

Line 11-13: If the set of network junctions without cycle \mathcal{V}_J is empty, the algorithm terminated since adding further cycles is not possible and higher benefit cannot be achieved. The resulting graph consists of the source node \mathcal{V}_S , the network junctions without cycle \mathcal{V}_J , the network junctions with a cycle \mathcal{V}_C and the exit nodes \mathcal{V}_E .

Line 14: If no exit condition was satisfied, the routine is repeated for the new graph that consists of the source node \mathcal{V}_S , the network junctions without cycle \mathcal{V}_J , the network junctions with a cycle \mathcal{V}_C and the exit nodes \mathcal{V}_E .

Note that *Algorithm 1* terminates after a finite number of steps. The result of *Algorithm 1* is feasible for the optimal design and control problem

$$\min_{(p_0,\varepsilon)} f(p_0,\varepsilon) \quad \text{s.t.} \quad \varepsilon \ge 0, \ p_0 \ge 0, \tag{4.2}$$

where the cost function is given by

$$f: \mathbb{R} imes \mathbb{R}^{|\mathscr{V}_J|} o \mathbb{R}, \qquad f(p_0, oldsymbol{arepsilon}) = oldsymbol{\omega}_0(p_0 - ar{p}_0)^2 + \sum_{i \in \mathscr{V}_E} oldsymbol{\omega}_i(p_i(p_0, oldsymbol{arepsilon}) - ar{p}_i)^2.$$

So instead of solving the optimal design and control problem (4.2), which requires enormous numerical effort for large graphs, *Algorithm 1* provides a strategy to obtain a feasible solution with low control cost. A numerical example for the tree-structured graph shown in *Figure 7* is provided in the *Appendix*.

5. Conclusions

In this paper, we analyzed the problem of finding the optimal shape and control for gas networks. Based on the assumption that a turnpike property holds for the dynamic optimal control problem, we replaced the gas dynamics by a stationary model, enabling the presence of an explicit solution for the pressure and the flow on the network. In *Section 2*, we laid the groundwork for our analysis: The numerical study of a turnpike result for the gas dynamics on networks. In *Section 3*, we presented the analysis for the explicit solution on a network junction.

We computed the topological derivative for the network junction, while a negative value for the topological derivative means that replacing the center node with a small cycle improves the network in terms of cost. We also analyzed the optimal design and control problem as a bilevel problem, in which control problem (depending on the cycle size) was solved on the lower level, enabling us to solve the optimal shape problem depending on the optimal control. Based on this analysis, in *Section 4*, we presented a strategy to find the optimal shape and control of a network by considering the network junctions individually, allowing us to exploit the analysis presented before.

An extension of our approach is possible in various directions. It can also be applied to tree-structured gas networks with an arbitrary number of source nodes. Then, computing the explicit solution as we did in (3.10), (3.11) is more challenging, but still possible, and *Algorithm 1* can be applied as well. Considering arbitrary gas networks is also possible, but due to the lack of an explicit solution for the pressure, *Algorithm 1* can only be performed numerically, without exploiting the explicit solution. This means that a new strategy to solve the control problem on the lower level and the shape problem on the upper level has to be developed, since the lower level cannot be replaced by the root of the control cost, c.f., (3.18).

A natural next step is the analysis of the turnpike phenomenon for the semi-linear gas model. Although there exist various turnpike results for linear problems, the number of turnpike results for the nonlinear case is rather limited, especially in the context of hyperbolic PDEs. However, the turnpike phenomenon for nonlinear hyperbolic systems deserves further attention, since it is interesting and challenging. Without the turnpike assumption from *Section 2*, it becomes necessary to analyze the control and shape problem for the gas dynamics, which was, to our best knowledge, not considered yet.

Acknowledgments

Deutsche Forschungsgemeinschaft (DFG) in the Collaborative Research Centre CRC/Transregio 154, Mathematical Modelling, Simulation and Optimization using the Example of Gas Networks, Project C03, Projektnummer 239904186.

REFERENCES

- [1] U.S. Energy Information Administration, International Energy Outlook 2018, U.S. Department of Energy, 2018, https://www.eia.gov/outlooks/ieo/executive_summary.php.
- [2] FNB Gas, Hydrogen Network 2030: towards a climate-neutral Germany, 2021, https://fnb-gas.de/wasserstoffnetz/h2-netz-2030/#_ftnref1.
- [3] European Hydrogen Backbone, Five Hydrogen Supply Corridors for Europe in 2030, 2022, https://ehb.eu/page/publications.
- [4] M. Banda, M. Herty, A. Klar, Gas flow in pipeline networks, Netw. Hererog. Media 1 (2006), 41–56.
- [5] M. Gugat, S. Ulbrich, Lipschitz solutions of initial boundary value problems for balance laws, Math. Models Methods Appl. Sci. 28 (2018), 921–951.
- [6] A. Osiadacz, Simulation and Analysis of Gas Networks, E & F.N. Spon, London, 1987.
- [7] M. Schuster. Nodal Control and Probabilistic Constrained Optimization using the Example of Gas Networks. Dissertation, FAU Erlangen-Nürnberg, Germany (2021), https://opus4.kobv.de/opus4-trr154/frontdoor/index/index/docId/410.
- [8] M. Banda, M. Herty, A. Klar, Coupling conditions for gas networks governed by the isothermal Euler equations, Netw. Heterog. Media 1 (2006), 295–314.

- [9] T. Koch, B. Hiller, M. E. Pfetsch, L. Schewe, Evaluating Gas Network Capacities, MOS-SIAM, Philadelphia, 2015.
- [10] P. Domschke, B. Hiller, J. Lang, C. Tischendorf, Modellierung von Gasnetzwerken: Eine Übersicht, Technical Report 2717, Technische Universität Darmstadt, 2017, http://www3.mathematik.tu-darmstadt.de/fb/mathe/preprints.html.
- [11] E. Cavalheiro, A. Vergílio, C. Lyra, Optimal configuration of power distribution networks with variable renewable energy resources, Comput. Oper. Res. 96 (2018), 272–280.
- [12] S. Göttlich, R. Korn, K. Lux-Gottschalk, Optimal control of electricity input given an uncertain demand, Math. Mathods Oper. Res. 90 (2019), 1–28.
- [13] J. Wu, Z. Gao, H. Sun, Optimal traffic networks topology: A complex networks perspective, Phys. A: Stat. Mech. Appl. 387 (2008), 1025–1032.
- [14] S. Göttlich, M. Herty, U. Ziegler, Modeling and optimizing traffic light settings in road networks, Comput. Oper. Res. 55 (2015), 36–51.
- [15] O. Stein, G. Still, T. Terlaky, G. Weber, Time-Varying Network Optimization, Springer, New York, 2008.
- [16] M. Saad, T. Terlaky, A. Vannelli, H. Zhang, Packing Trees in Communication Networks, In: X. Deng, Y. Ye (eds) Internet and Network Economics, WINE 2005, Lecture Notes in Computer Science, vol. 3828, Springer, Berlin, Heidelberg, 2005.
- [17] M. Gugat, F. Hante, M. Hirsch-Dick, G. Leugering, Stationary States in Gas Networks, Netw. Heterog. Media 10 (2015), 295–320.
- [18] C. Gotzes, H. Heitsch, R. Henrion, R. Schultz, On the quantification of nomination feasibility in stationary gas networks with random load, Math. Methods Oper. Res. 84 (2016), 427–457.
- [19] M. Gugat, M. Schuster, Stationary gas networks with compressor control and random loads: Optimization with probabilistic constraints, Math. Prob. Eng. 2018 (2018), 7984079.
- [20] S. Srinivasan, K. Sundar, V. Gyrya, A. Zlotnik, Numerical solution to the steady state network flow equations for a nonideal gas, IEEE Trans. Control Netw. Syst. 10 (2022), 1449–1461.
- [21] J. Sokolowski, A. Zochowski, On the topological derivative in shape optimization, SIAM J. Control Optim. 37 (1999), 1251–1272.
- [22] G. Leugering, J. Sokolowski, Topological sensitivity analysis for elliptic problems on graphs, Control Cybernet. 37 (2008), 971–997.
- [23] A. Porretta, E. Zuazua, Long Time versus Steady State Optimal Control, SIAM J. Control Optim. 51 (2013), 4242–4273.
- [24] E. Trélat, E. Zuazua, The turnpike property in finite-dimensional nonlinear optimal control, J. Differential Equations 258 (2015), 81–114.
- [25] A. Zaslavski, Turnpike Properties in the Calculus of Variations and Optimal Control, Springer, New York, 2006.
- [26] M. Gugat, F. Hante, On the Turnpike Phenomenon for Optimal Boundary Control Problems with Hyperbolic Systems, SIAM J. Control Optim. 57 (2019), 264–289.
- [27] N. Sakamoto, M. Schuster, A turnpike result for optimal boundary control problems with the transport equation under uncertainty, Math. Control Signals Syst. (2025), https://doi.org/10.1007/s00498-025-00422-y.
- [28] L. Grüne, R. Guglielmi, Turnpike Properties and Strict Dissipativity for Discrete Time Linear Quadratic Optimal Control Problems, SIAM J. Control Optim. 56 (2018), 1282–1302.
- [29] L. Grüne, L. Krügel, Local Turnpike Analysis using Local Dissipativity for Discrete Time Discounted Optimal Control, Appl. Math. Optim. 84 (2021), 1585–1606.
- [30] T. Faulwasser, K. Flaßkamp, S. Ober-Blöbaum, M. Schaller, K. Worthmann, Manifold Turnpikes, Trims, and Symmetries, Math. Control Signals Syst. 34 (2022), 759–788.
- [31] A. Zaslavski, Existence and Structure of Optimal Solutions of Infinite-Dimensional Control Problems, Appl. Math. Optim. 42 (2000), 291–313.
- [32] T. Faulwasser, L. Grüne, Turnpike Properties in Optimal Control: An Overview of Discrete-Time and Continuous-Time Results, In: Handbook of Numerical Analysis, Numerical Control: Part A, vol. 23, pp. 367–400, Elsevier, Amsterdam, 2022.

- [33] M. Gugat, S. Ulbrich, The Isothermal Euler Equations for Ideal Gas with Source Term: Product Solutions, Flow Reversal and no Blow up, J. Math. Anal. Appl 454 (2017), 439–452.
- [34] M. Gugat, J. Sokolowski. On problems of dynamic optimal nodal control for gas networks, Pure Appl. Funct. Anal. 7 (2022), 1699–1715.
- [35] R. Fourer, D. Gay, B. Kernighan, AMPL A Modeling Language for Mathematical Programming, Second Edition, Duxbury, 2002.
- [36] M. Schmidt, M. Steinbach, B. Willert, High Detail Stationary Optimization Models for Gas Networks: Validation and Results, Optim. Eng. 16 (2014), 437–472.
- [37] S. Kazi, K. Sundar, S. Srinivasan, A. Zlotnik, Modeling and Optimization of Steady State Flow of Natural Gas and Hydrogen Mixtures in Pipeline Networks, Int. J. Hydrog. Energy 54 (2024), 14–24.
- [38] M. Gugat, R. Schultz, M. Schuster, Convexity and starshapedness of feasible sets in flow networks, Netw. Heterog. Media 15 (2020), 171–195.

APPENDIX: A NUMERICAL EXAMPLE FOR ALGORITHM 1

We provide a numerical example for *Algorithm 1* applied to the tree-structured graph shown in *Figure 7* here. The network topology is shown in *Table 2*. The outflows for the exit nodes in \mathcal{V}_E are given by

$$b = \begin{bmatrix} 50 & 20 & 80 & 60 & 30 & 50 & 40 & 20 \end{bmatrix} \frac{\text{kg}}{\text{m}^2 \text{s}}.$$

Pipe friction, pipe diameter, temperature, and specific gas constant are given by

$$\lambda = 0.05$$
, $D = 0.5 \text{ m}$, $T = 10^{\circ}\text{C}$ and $R_S = 519.66 \frac{J}{kg K}$,

where the latter is defined by the properties of methane. Further, we set

$$\omega_0 = \omega_i = 1 \quad \forall i \in \{1, 2, 3, 5, 7, 8, 10\},$$

and for the reference pressures, we set

$$\bar{p}_0 = 55 \text{ bar}$$
 and $\bar{p} = \begin{bmatrix} 40 & 50 & 45 & 48 & 46 & 45 & 48 & 49 \end{bmatrix} \text{ bar}$.

For $p_0 = 60$ bar, the objective value for the network without a cycle is given by

$$f(p_0,0) = 30.9536.$$

source node	set of network junctions	set of exit nodes
$\mathcal{V}_S = \{v_0\}$	$\mathcal{V}_J = \{v_1, v_2, v_3, v_5, v_7, v_8, v_{10}\}$	$\mathcal{V}_E = \{v_4, v_6, v_9, v_{11}, v_{12}, v_{13}, v_{14}, v_{15}\}$

TABLE 2. Source nodes, network junctions and exit nodes for the graph shown in *Figure 7*.

Algorithm 1: First Iteration. We successively add a cycle to every network junction and solve the corresponding optimal control problem (*Line 2*), and we compute the topological derivative for every cycle (*Line 3*), which are shown in *Table 3*. We set $v^* := v_2$, since $\mathcal{T}_{J_2}(v_2)$

TABLE 3. Topological Derivative for a cycle at network junction v_j in the first iteration.

is the smallest derivative. The solution of the optimal design problem (4.1) is given by

$$\varepsilon_2^* = 1523.0205 \text{ m}, \qquad p_0^*(\varepsilon_2^*) = 58.9968 \text{ bar} \qquad \text{and} \qquad J_2(\varepsilon_2) = 19.048.$$

Thus we add a cycle with length ε_2^* at node v_2 , and we set

$$\mathcal{V}_J = \{v_1, v_3, v_5, v_7, v_8, v_{10}\}$$
 and $\mathcal{V}_C = \{v_2\},$

which is shown in *Figure 9*.

Algorithm 1: Second Iteration. We successively add a cycle to every remaining network junction and solve the corresponding optimal control problem (Line 2), and we compute the topological derivative for every cycle (*Line 3*), which are shown in *Table 4*. We set $v^* := v_3$,

ond iteration.

since $\mathcal{T}_{J_3}(v_3)$ is the smallest derivative. The solution of optimal design problem (4.1) is given by

$$\varepsilon_3^* = 2866.2292 \text{ m}, \text{ and } p_0^*(\varepsilon_3^*) = 58.9095 \text{ bar} \quad \text{and} \quad J_3(\varepsilon_3^*) = 18.7068.$$

Thus we add a cycle with length ε_3^* at node v_2 , and we set

$$\mathcal{V}_J = \{v_1, v_5, v_7, v_8, v_{10}\}$$
 and $\mathcal{V}_C = \{v_2, v_3\},$

which is shown in *Figure 10*.

Algorithm 1: Third Iteration. We successively add a cycle to every remaining network junction and solve the corresponding optimal control problem (Line 2), and we compute the topological derivative for every cycle (*Line 3*), which are shown in *Table 5*. We set $v^* := v_1$,

TABLE 5. Topological Derivative for a cycle at network junction v_i in the second iteration.

since $\mathcal{T}_{J_1}(v_1)$ is the smallest derivative. The solution of the optimal design problem (4.1) is given by

$$\varepsilon_1^* = 592.8666$$
 m, and $p_0^*(\varepsilon_1^*) = 58.8963$ bar and $J_1(\varepsilon_1^*) = 18.6118$. we add a cycle with length ε_1^* at node v_2 and we set

Thus we add a cycle with length ε_1^* at node v_2 and we set

$$\mathcal{V}_J = \{v_5, v_7, v_8, v_{10}\}$$
 and $\mathcal{V}_C = \{v_1, v_2, v_3\},$

which is shown in *Figure 11*.

Algorithm 1: Fourth Iteration. We successively add a cycle to every remaining network junction and solve the corresponding optimal control problem (Line 2), and we compute the topological derivative for every cycle (Line 3), which are shown in Table 6. Since all topological

j	5	7	8	10
$10^4 \cdot \mathcal{T}_{J_i}(v_j) =$	-0.0000	-0.0000	-0.0000	-0.0000

TABLE 6. Topological Derivative for a cycle at network junction v_j in the second iteration.

derivatives are close to machine accuracy, the exit condition (*Line 5,6*) is met and *Algorithm 1* finished. In every step, we can observe a decrease of the cost $J(\varepsilon)$. Thus, *Algorithm 1* provides a network with three cycles $\varepsilon_1^*, \varepsilon_2^*, \varepsilon_3^*$ and the corresponding optimal control $p_0^*(\varepsilon_1^*)$ with low control cost.

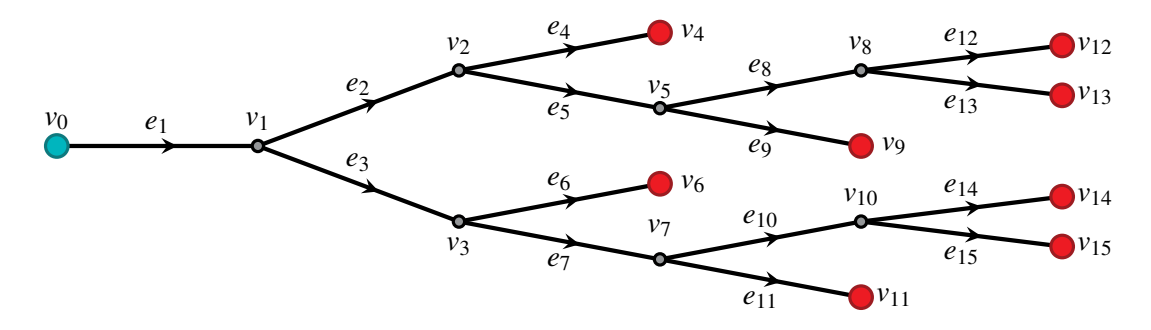


FIGURE 8. Initial Graph before applying *Algorithm 1*.

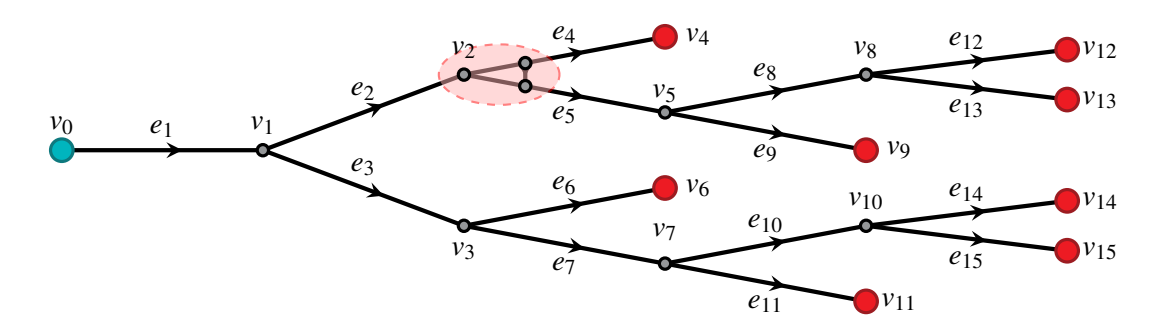


FIGURE 9. Graph after one iteration of *Algorithm 1*.

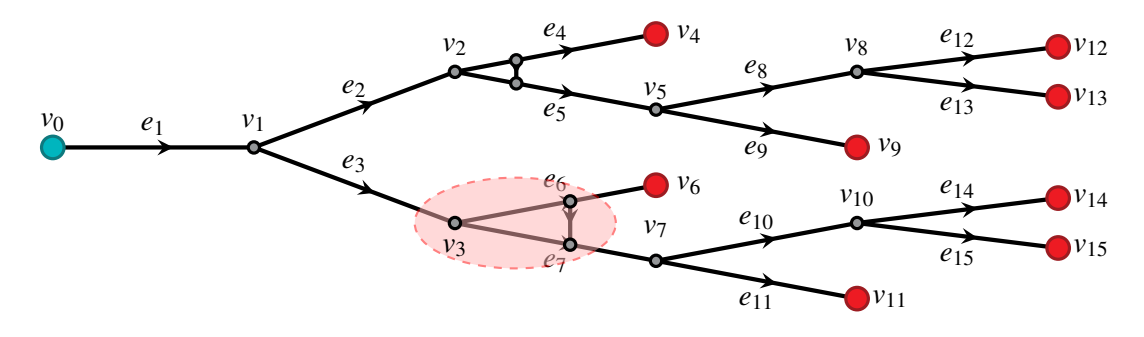


FIGURE 10. Graph after two iterations of *Algorithm 1*.

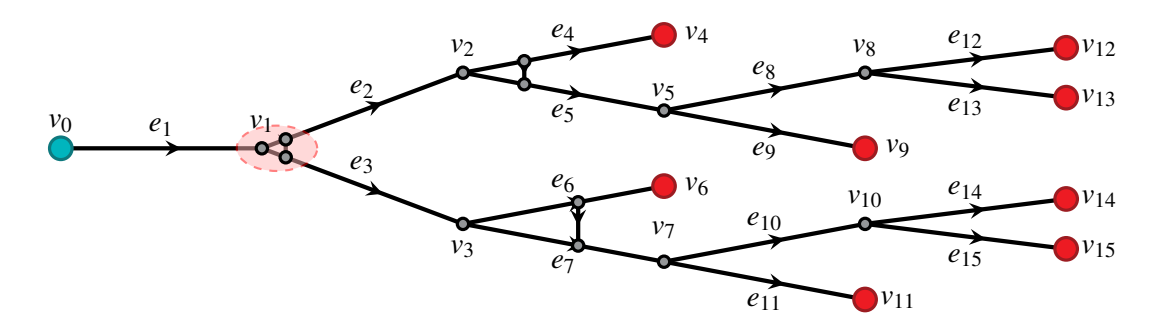


FIGURE 11. Graph after three iterations of *Algorithm 1*.